



RESEARCH ARTICLE

PROPERTIES OF SOL-GEL DERIVED SILVER DOPED TITANIA NANOPARTICLES

<sup>1</sup>\*Rajamannan, B., <sup>1</sup>Mugundan, S., <sup>2</sup>Viruthagiri, G., <sup>2</sup>Shanmugam, N. and <sup>2</sup>Praveen, P.

<sup>1</sup>Department of Engineering Physics, (FEAT), Annamalai University, Annamalainagar-608002

<sup>2</sup>Department of Physics, Annamalai University, Annamalainagar-608002

ARTICLE INFO

Article History:

Received 08<sup>th</sup> July, 2013

Received in revised form

10<sup>th</sup> August, 2013

Accepted 14<sup>th</sup> September 2013

Published online 10<sup>th</sup> October, 2013

Key words:

Sol-gel;

silver-doped TiO<sub>2</sub>;

Crystalline size,

FT-IR; DRS;

PL; SEM.

ABSTRACT

Silver doped (4%, 8%, 12% and 16%) TiO<sub>2</sub> nanoparticles have been prepared by sol-gel method at room temperature. In this present study, we used titanium tetra isopropoxide and 2-propanol as a common starting materials and found that the final product was in anatase phase. The samples of pure anatase were calcined at 500°C for 5 h. The X-ray powder diffraction study reveals that all the prepared samples have pure anatase phase of tetragonal system. The functional groups of the samples were identified by Fourier transform infrared spectroscopy (FT-IR). The diffused reflectance UV-Vis-DRS spectra indicated that the Ag doped TiO<sub>2</sub> samples exhibit higher blue shifts compared with the undoped TiO<sub>2</sub> nanoparticle. The photoluminescence studies showed that emission Peaks are shifted to lower wavelength regions. The morphological structures and elements present in the samples were determined by using techniques viz., scanning electron microscopy (SEM) with energy dispersive x-ray analysis (EDX).

Copyright © 2013 Rajamannan, et al., This is an open access article distributed under the Creative Commons Attribution License, which permits unrestricted use, distribution, and reproduction in any medium, provided the original work is properly cited.

INTRODUCTION

Titanium dioxide owing to high photocatalytic activity, chemical stability, availability, non-toxicity, low price and fast electron transfer to molecular oxygen has attracted considerable attention as a photo catalyst for the degradation of organic pollutants [1]. The TiO<sub>2</sub> exists mostly as rutile and anatase phases which both of them have the tetragonal structures. Among these polymorphs, rutile and anatase have been widely studied. Brookite is rarely studied due to its complicated structure and difficulties in sample preparation [2]. In the past decades, metal-doped TiO<sub>2</sub> nanoparticles have attracted much attention, because introduction of metal ions could enhance the photo catalytic activity of TiO<sub>2</sub> drastically in some cases. Generally, the accepted mechanism to explain the enhancement is the formation of shallow charge trapping on the surface of TiO<sub>2</sub> nanoparticles due to the replacement of Ti<sup>4+</sup> by metal ions [3]. Titanium dioxide is a semiconductor material has long been studied as a photocatalyst in energy and environmental applications due to its high photocatalytic activity, photosensitivity, non-toxicity and physical and chemical stability. Photocatalysis occurs when a photocatalyst is exposed to photons with at least as much energy as the band gap energy of the photocatalyst [4]. Semiconductor Nanoparticles have attracted a great deal of attention due to their potential application in solar energy conversion, dielectric, etc.

TiO<sub>2</sub> is believed to be most promising currently known materials due to its excellent optical properties of a high refractive index leading to a high hiding power and whiteness. Among several oxide semiconductors, titanium dioxide has a more helpful role in our environmental purification due to its non-toxicity, photo catalytic activity, photo induced super-hydrophilicity and antifogging effect [5]. Titanium dioxide has a wide band-gap of 3.2eV, which can be activated under ultraviolet light. It exists in three polymorphic phases: anatase, rutile and brookite. Among them, the anatase phase has the highest photocatalytic activity compared with the rutile and brookite phases. However, the rutile structure is the most stable form at high temperature, and anatase and brookite both can be converted to rutile upon heating [6]. Doping metal onto TiO<sub>2</sub> has been proved an effective strategy to improve the catalytic process. Sol-gel process is one of the methods generally employed for the preparation of TiO<sub>2</sub>. This method is very suitable for fabricating transparent film. Several researchers synthesized Ag/TiO<sub>2</sub> sol by adding silver compound to modify the sol-gel process [7]. Depending on the synthetic approach they used, TiO<sub>2</sub> samples with various physical and chemical properties were obtained. By the sol-gel method, one could obtain TiO<sub>2</sub> nanoparticles with high homogeneity, and particle size could be easily tuned [8].

MATERIALS AND METHODS

Sample preparation

Preparation of Bare and Silver doped TiO<sub>2</sub> nanopowder: Sol-gel technique was used to prepare bare and silver-doped TiO<sub>2</sub>

\*Corresponding author: Rajamannan, Department of Engineering Physics, (FEAT), Annamalai University, Annamalainagar-608002.

samples. 90 ml of 2-propanol was taken as primary precursor and 10 ml Titanium tetra isopropoxide was added to it drop wise with stirring during the process of  $\text{TiO}_2$  formation. The solution was vigorously stirred for 45 min in order to form sols. Liquid solution silver nitrate of different concentrations (4%, 8%, 12% and 16%) was poured slowly drop by drop to that mixture with continued stirring. In order to obtain nanoparticles, the gels were dried at  $80^\circ\text{C}$  for 5 h to evaporate water and organic material to the maximum extent. Then the dry gel was calcined at  $500^\circ\text{C}$  for 2 h to obtain desired anatase  $\text{TiO}_2$  nanoparticles.

### Sample characterization

The bare and Ag doped  $\text{TiO}_2$  anatase are subjected into different characterizations, such as powder XRD, FTIR, UV-DRS, PL and SEM with EDX. The crystalline phase and particle size of  $\text{TiO}_2$  nanoparticles were analyzed by X-ray diffraction (XRD) measurement, which was carried out at room temperature by using XPERT-PRO diffractometer system (scan step of  $0.05^\circ$ , counting time of 10.16 s per data point) equipped with a Cu tube for generating  $\text{CuK}\alpha$  radiation ( $\lambda = 1.5406 \text{ \AA}$ ). The incident beam in the 2-theta mode over the range of  $10^\circ$ – $80^\circ$ , operated at 40 kV and 30 mA. The chemical structure was investigated by AVATAR 330 Fourier transform infrared spectrometer (FTIR) in which the IR spectrum was recorded by diluting the mixed powder in KBr and in the wavelength between  $4000$ – $400 \text{ cm}^{-1}$  was used to assess the presence of functional groups in  $\text{TiO}_2$ . The diffuse reflectance spectra (DRS) was measured at wavelength in the range of  $200$ – $800 \text{ nm}$  by UV-Vis-NIR spectrophotometer (Varian/Carry 5000) equipped with an integrating sphere and the baseline correction was performed using a calibrated reference sample of powdered barium sulphate ( $\text{BaSO}_4$ ). The photoluminescence spectra (PL) are recorded with Perkin Elmer LS fluorescence spectrophotometer. Scanning electron microscope (SEM) images were observed with a Hitachi S-4800 microscope, combined with energy dispersive X-ray spectroscopy (EDX, Oxford 7021) for determination of elemental composition.

## RESULTS AND DISCUSSION

### X-Ray Diffraction

Figure 1 shows the X-ray diffraction of the bare and Ag doped  $\text{TiO}_2$  nanoparticles after calcined at  $500^\circ\text{C}$  for 5 hr. X-ray diffraction studies indicate that the materials synthesized are pure anatase  $\text{TiO}_2$  phase and the tetragonal structures and well agree with the corresponding reported JCPDS value (JCPDS card no. 21-1272). We did not observe any peaks corresponding to Rutile and Brookite phases [9]. The XRD pattern of  $\text{TiO}_2$  shows five primary peaks at  $25.2^\circ$ ,  $38^\circ$ ,  $48.2^\circ$ ,  $55^\circ$  and  $62.5^\circ$  which can be attributed to different diffraction planes of anatase phase  $\text{TiO}_2$  [10]. However, various diffraction lines of  $\text{TiO}_2$  corresponding to anatase phase can be clearly seen for all the samples. Metallic silver particles exhibited strong peaks at  $38^\circ$  (111),  $55^\circ$  (006), and  $76^\circ$  (114) indicating the Ag attachment to the  $\text{TiO}_2$  surface [11]. The Ag doped  $\text{TiO}_2$  nanoparticles clearly exhibit the diffraction peaks of the metallic silver and showed a face centered cubic structure of metallic silver. From the obtained peak the average nanocrystalline sizes was measured according to Debye-Scherrer formula (eqn. 1) and are presented in Table 1.

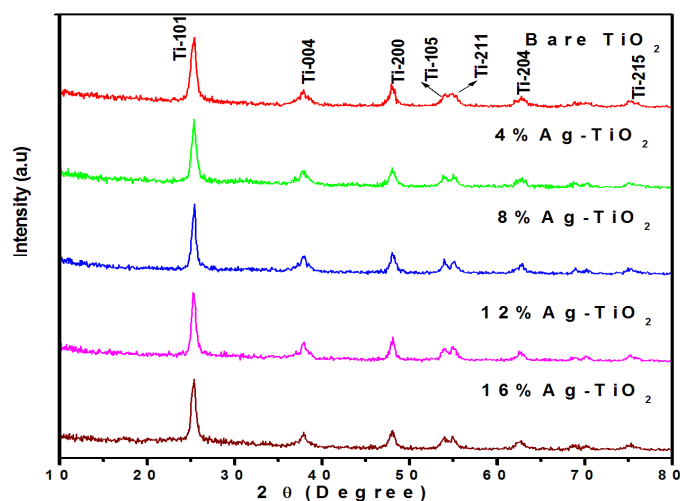


Fig.1. X-Ray diffraction pattern for bare  $\text{TiO}_2$  and Ag doped  $\text{TiO}_2$  nanoparticles

Table 1: Crystallite sizes for the bare and Ag doped  $\text{TiO}_2$  nanoparticles

Samples	Crystallite size (nm)
Bare $\text{TiO}_2$	15.31
4% Ag doped $\text{TiO}_2$	9.40
8% Ag doped $\text{TiO}_2$	12.19
12% Ag doped $\text{TiO}_2$	15.10
16% Ag doped $\text{TiO}_2$	9.63

$$D = \frac{K\lambda}{\beta \cos\theta} \rightarrow 1$$

Where, D - Crystallite size, K - Shape factor,  $\lambda$  -  $0.154 \text{ nm}$ ,  $\beta$  - Full width at half maximum and  $\theta$  - Reflection angle. Line broadening of the diffraction peaks is an indication that the synthesized particles are in the range of  $9.4$  -  $15.30 \text{ nm}$ . It is important to indicate that crystallite size is increasing in doping concentration and when compared to the pure  $\text{TiO}_2$ , doping of Ag was found to decrease the  $\text{TiO}_2$  crystallite size.

### Fourier Transform Infrared Spectroscopy

Fig. 2 shows the FTIR spectra of the obtained bare and Ag doped  $\text{TiO}_2$  nanoparticles after calcined at  $500^\circ\text{C}$  for 5 h. It was absorbed that the strong band in the range of  $900$ – $500 \text{ cm}^{-1}$  is associated with the characteristic vibrational modes of  $\text{TiO}_2$ . This confirms that the  $\text{TiO}_2$  phase has been formed [12]. The absorption band at  $1,629 \text{ cm}^{-1}$  was due to the presence of O–H bending vibration which is probably because of the reabsorption of water from the atmosphere [13]. The absorption bands at  $3,419 \text{ cm}^{-1}$  is attributed to the presence of O–H stretching [14]. The peaks in between  $2924$  and  $2843 \text{ cm}^{-1}$  are assigned to C–H stretching vibrations of alkane groups. The alkane and carboxylate group come from Titanium tetra isopropoxide and 2-propanol, which we used in the synthesis process. The sharp peak corresponding to  $1,630 \text{ cm}^{-1}$  is observed in the deformation region for molecular water, which can be attributed to the H–O–H bending vibration ( $\gamma \text{ OH}$ ) of the physisorbed or free water molecule that is strongly bound to the catalyst surface [15]. The broad, strong IR peak at about  $3,430 \text{ cm}^{-1}$  is assigned to the stretching  $\gamma \text{ OH}$  vibrations of the surface hydroxyl groups; it is often believed that the  $\text{TiO}_2$ -OH bonds arise from the hydrolysis reaction in the sol-gel process

[16]. These peaks are strongly confirming the presence of hydroxyl ions in the structure of the samples. When the doping concentration was increased, no other peaks were formed. The obtained FT-IR results are in good agreement with the XRD analysis and no alkoxy groups are present in the samples.

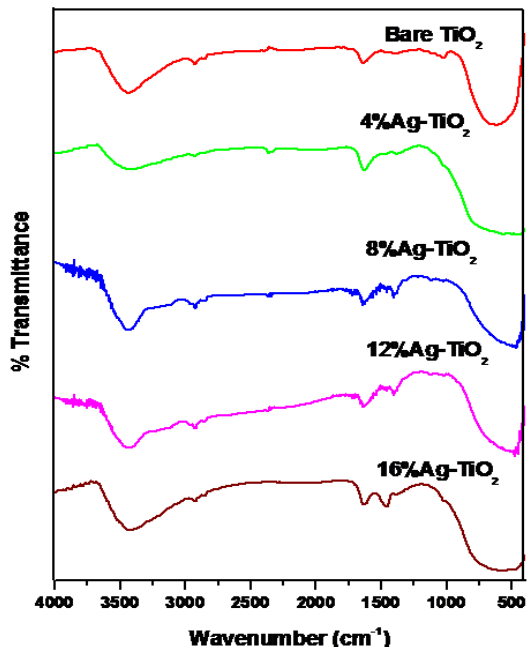


Fig.2. FTIR spectra for bare TiO₂ and Ag doped TiO₂ nanoparticles

Ultra Violet- Diffuse Reflectance Spectra

The optical properties of samples were characterized by UV-DRS. The diffused reflectance spectra of undoped and different weight percentages (4 %, 8%, 12%, and 16%) of Silver doped TiO₂ were shown in Fig.3.

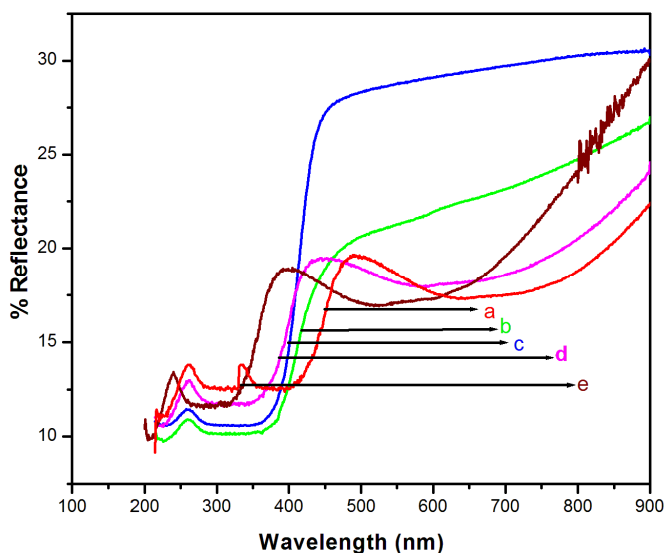


Fig.3. UV-DRS spectra for bare TiO₂ and Ag doped TiO₂ nanoparticles (a-Bare TiO₂, b-4%Ag-TiO₂, c-8%Ag-TiO₂, d-12%Ag-TiO₂, e-16%Ag-TiO₂)

The spectrum of TiO₂ consists of a single absorption below 370 nm usually ascribed to charge-transfer from the valence band (mainly formed by 2p orbitals of the oxide anions) to the conduction band (mainly formed by 3d<sub>t2g</sub> orbitals of the Ti<sup>4+</sup>

cations) [17,18]. The absorption edge shifts towards shorter wavelengths for the Ag doped TiO₂ catalysts, indicating an increase in the band gap energies of TiO₂ with increasing amount of silver. After doping with silver ions the response of TiO₂ nanoparticles to visible light was increased and showed blue shift (towards decreased wavelength). The blue shift of the absorption curve results in a reduction of the band gap energy and the recombination rate, and hence, enhanced photocatalytic activity. The band gap energies were calculated from the cut off wavelength of bare and Ag doped TiO₂. The calculated values are 3.58 eV (345 nm), 3.62 eV (340 nm), 3.75 eV (330 nm), 3.86 eV (321 nm) and 3.93 eV (315 nm). The band gap energy (E<sub>g</sub>) of bare TiO₂ was obtained from the wavelength value corresponding the spectrum, using the (eqn. 2)

$$E_g = \frac{hc}{\lambda} \quad ; \quad \lambda = \frac{hc}{E_g} \quad \text{-----} \rightarrow 2.$$

The energy band gap corresponds to the absorption limit and can be roughly evaluated by the above relation. Where, E<sub>g</sub> - band gap energy (eV), h - Planck’s constant (6.626×10<sup>-34</sup> Js), c - Light velocity (3×10<sup>8</sup> m/s) and λ - Wavelength (nm). However, after various levels of Silver doping the band gap is lying between 3.58 eV and 3.93 eV respectively as shown in Table 2. This increased band gap is to be more photoreactive and result in its usage in visible light [19]. The spectra reveal that Ag doping has a marked effect on the absorption properties of TiO₂ and that the absorption of light in the visible region by TiO₂ increases with an increase in the silver content.

Table 2. Band gap energy for bare and Ag doped TiO₂ nanoparticles

Samples	Band gap (eV)
Bare TiO₂	3.58
4% Ag doped TiO₂	3.62
8% Ag doped TiO₂	3.75
12% Ag doped TiO₂	3.86
16% Ag doped TiO₂	3.92

Photoluminescence

The Fig.4 shows the PL emission spectra of bare and Ag doped TiO₂ nanoparticles.

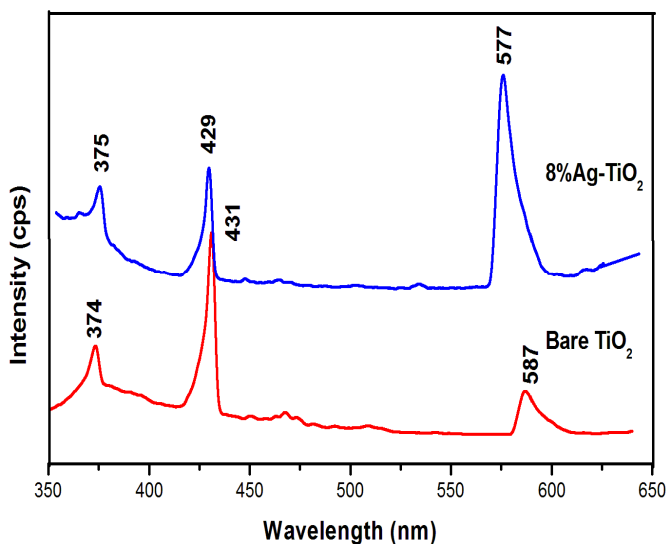


Fig.4. PL spectra for bare TiO₂ and Ag doped TiO₂ nanoparticles

The excited wavelength is 350 nm, respectively for bare and Silver (8%) doped TiO<sub>2</sub>. The emission bands originating from the excited level was monitored in the spectral region between 350-650 nm. The energy of the trap level was identified at 587 nm is attributed to Ti<sup>4+</sup> ions adjacent to oxygen vacancies (intra gap surface states) [20]. The UV emission is considered as the band edge emission of the host TiO<sub>2</sub>, and the 431 nm peak can be ascribed to self-trapped excitons localized in TiO<sub>6</sub> octahedra [21]. A band at 373 nm is attributed to the first vibronic fluorescence band (i.e. symmetry forbidden 0-0 band (I<sub>1</sub>)) [22]. When compared with bare TiO<sub>2</sub> the PL emission spectrum of 8% Ag doped TiO<sub>2</sub> nanoparticles show the three peaks (375, 429 and 577 nm). The peak at 577 nm is sharp and broad with high intensity compare to bare TiO<sub>2</sub> nanoparticle. The peak at 429 nm is low intensity compare to 431 nm bare TiO<sub>2</sub>. The peaks that were existing in bare TiO<sub>2</sub>, were blue shifted as result of doping.

### Scanning Electron Microscopy

Fig 5a & 6a show the SEM micrograph of bare and 8% Ag doped TiO<sub>2</sub> nanoparticles. From the figures, it can be observed that the particles sizes are spherical in shape with uniform size distribution [23, 24]. It can be seen that the average particle size of bare and 8% Ag doped TiO<sub>2</sub> nanoparticles is 9.63–15.30 nm and 8% Ag doping in the sol-gel method has little influence on the particle size of TiO<sub>2</sub>. From this micrograph, uniform distribution of particles is found.

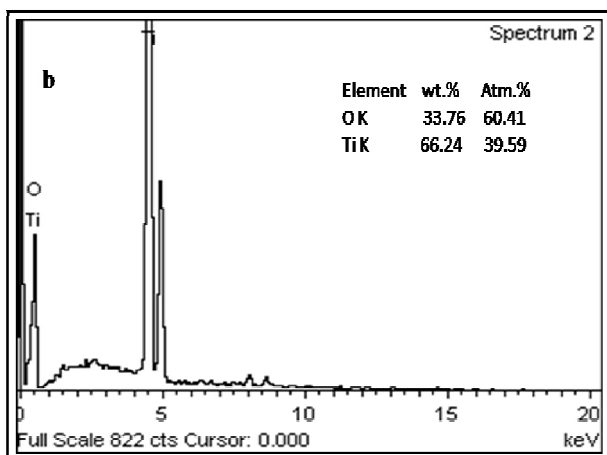
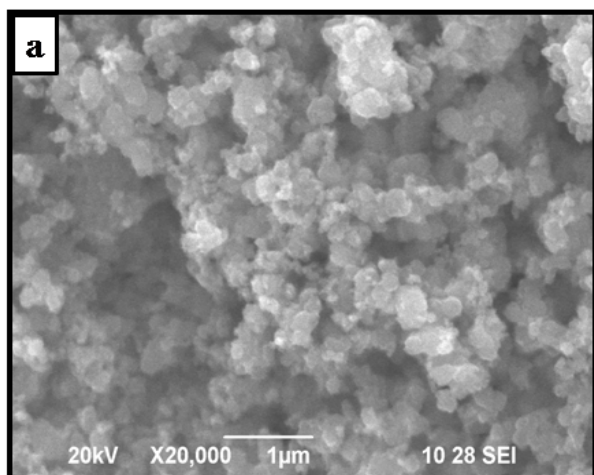


Fig.5. SEM Micrograph of TiO<sub>2</sub> nanoparticles (a) and corresponding to EDX diagram (b)

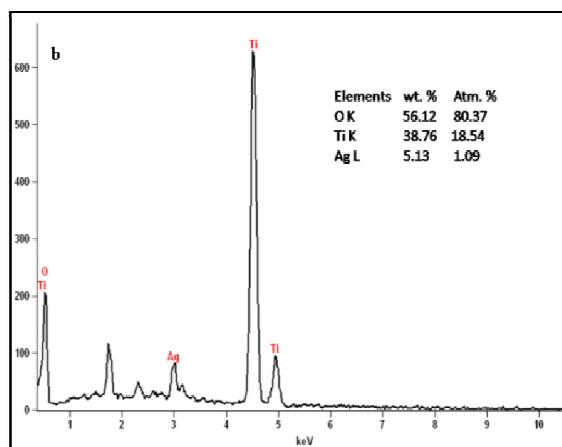
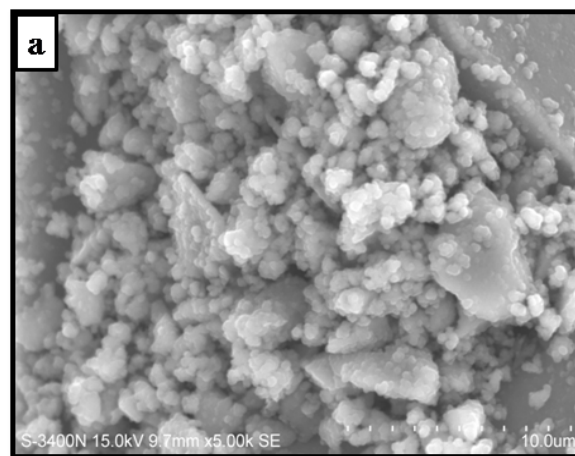


Fig.6. SEM Micrograph of Ag doped TiO<sub>2</sub> nanoparticles (a) and corresponding to EDX diagram (b)

They consist of either some single particles or clusters of particles. Energy-dispersive X-ray spectroscopy (EDX) of bare and 8% of Ag doped TiO<sub>2</sub> are shown in Figs.5b and 6b. The atomic ratios of Ag, Ti, and O are also listed in figs. 5b and 6b TiO<sub>2</sub> Figs.5c and 6c shows the presence of O, Ti and silver according to atomic weight of 80.37%, 18.54% and 1.09%, respectively [25].

### Conclusions

The bare and Ag (4%, 8%, 12% & 16%) doped TiO<sub>2</sub> nanoparticles were successfully synthesized by Sol-gel method at room temperature and annealed at 500°C for getting anatase phase. From the results of XRD patterns it is confirmed that the TiO<sub>2</sub> was in anatase phase with crystallite size of 9.4 - 15.30 nm. In XRD pattern, particle size decreases with increase in doping concentrations. The existence of functional group was identified by FT-IR analysis. The optical cut-off wavelengths of Ag doped TiO<sub>2</sub> were blue shifted towards the lower wavelength side, resulting larger band gap energies compared to pure TiO<sub>2</sub>. PL Spectra observed a broad and sharp range of emission spectra. The peaks, which were existing in bare TiO<sub>2</sub>, were blue shifted as result of doping. The SEM with EDX confirms the phase formation.

### REFERENCES

- [1] Yun Liu., Chun-yan Liu., Qing-hui Rong., Zhao Zhang. 2003. Characteristics of the silver-doped TiO<sub>2</sub> nanoparticles. Applied Surface Science, 220: 7–11.

- [2] Hu, W.B., Li, L.P., Li, G.S., Tang, C.L., Sun, L. 2009. High-Quality Brookite TiO<sub>2</sub> Flowers: Synthesis, Characterization, and Dielectric Performance. *Cryst. Growth. Des.*, 9: 3676–3682.
- [3] Mohammad, A., Behnajady., Hamed Eskandarloo., 2013. Silver and copper co-impregnated onto TiO<sub>2</sub> -P25 nanoparticles and its photocatalytic activity. *Chemical Engineering Journal*, 228: 1207–1213.
- [4] Seonghyuk Ko., Chandra K. Banerjee., Jagannathan Sankar. 2011. Photochemical synthesis and photocatalytic activity in simulated solar light of nanosized Ag doped TiO<sub>2</sub> nanoparticle composite. *Composites: Part B*, 42: 579–583.
- [5] Ashkarran, A.A. 2011. Antibacterial properties of silver-doped TiO<sub>2</sub> nanoparticles under solar simulated light. *Journal of Theoretical and Applied Physics*, 4: 1-8.
- [6] Jinrui Ding and Kyo-Seon Kim. 2012. Preparation of nanostructured TiO<sub>2</sub> thin films by aerosol flame deposition process. *Korean J. Chem. Eng.*, 29(1): 54-58
- [7] Jagadale, T.C., Takale S.P., Sonawane, R.S., Joshi, H.M., Patil, S.I., Kale, B.B., Ogale, S.B. 2008. *J. Phys. Chem. C*, 112: 14595–14602.
- [8] Bin Zhao., Yu-Wen Chen. 2011. Ag/TiO<sub>2</sub> sol prepared by a sol–gel method and its photocatalytic activity. *Journal of Physics and Chemistry of Solids*, 72:1312–1318.
- [9] Manorama, S.V., Naveen Lavanya Latha, J., Shashi Singh. 2007. Photo reduction of Silver on Bare and Colloidal TiO<sub>2</sub> Nanoparticles Nanotubes: Synthesis, Characterization, and Tested for Antibacterial Outcome Debanjan Guin. *J. Phys. Chem. C*, 111: 13393-13397.
- [10] Behnajady, M.A., Modirshahla, N., Shokri, M., Rad, B. 2008. Enhancement Of Photocatalytic Activity Of TiO<sub>2</sub> nanoparticles By Silver Doping: Photo deposition versus Liquid Impregnation Methods. *Global NEST Journal*, 10: 1-7.
- [11] Urate Virkutyte., Rajender S. Varma. 2012. Synthesis and visible light photoactivity of anatase Ag and garlic loaded TiO<sub>2</sub> Nano crystalline catalyst. *RSC Advances*, 2: 2399–2407.
- [12] Khanna, P.K., Singh, N., Charan, S. 2007. Synthesis of nanoparticles of anatase TiO<sub>2</sub> and preparation of its optical transparent film in PVA. *Mater. Lett.*, 61: 4725–4730.
- [13] Mohan, J. 2009. Organic spectroscopy principles and applications. 2<sup>nd</sup> edn. Narosha Publishing House Pvt. Ltd, New Delhi, pp 28–95.
- [14] Aziz, R.A., Sopyan, I. 2009. Synthesis of TiO<sub>2</sub> -SiO<sub>2</sub> powder and thin film photocatalysts of sol-gel method. *Int. J. Chem.*, 48: 951–957.
- [15] Ding, Z., Lu, G.Q., Greenfield, P.F. 2000. *J. Phys Chem B*, 104: 4815-4820.
- [16] Yeung, K.L., Yau, S.T., Maira, A.J., Coronado, J.M., Soria, J., Yue, P.L. 2003. Synthesis of TiO<sub>2</sub> based nanoparticles for photocatalytic applications. *J. Catal.*, 219: 107.
- [17] Gerischer, H., Heller, A. 1991. *J. Phys. Chem.*, 95: 5261-5266.
- [18] Sobana, N., Muruganadham, M., Swaminathan, M. 2006. Nano-Ag particles doped TiO<sub>2</sub> for efficient photo degradation of direct azo dyes. *J. Mol. Catal. A: Chem.*, 258: 124–132.
- [19] Narayana, R.L., Matheswaran, M., Aziz, A.A., Saravanan, P. 2011. Photocatalytic decolourization of basic green dye by pure and Fe, Co doped TiO<sub>2</sub> under daylight illumination. *Desal.*, 269: 249–253.
- [20] Abazovic, N.D., Mirjana, I., Omor, C., Anin, M.D.D., Jovanovic, D.J. 2006. Photoluminescence of Anatase and Rutile TiO<sub>2</sub> Particles. *J. Phys. Chem B.*, 110: 25366-25370.
- [21] Wan, W.Y., Chang, Y.M., Ting, J.M. 2010. Room-Temperature Synthesis of Single-Crystalline Anatase TiO<sub>2</sub> Nanowires *Cryst. Growth. Des.*, 10: 1646-1651.
- [22] Shown, I., Ujihara, M., Imae, T. 2010. *J. Colloid Interface Sci.*, 352: 232–237.
- [23] Reddy, M.V., Jose, R., Teng, T.H., Chowdari, B.V.R., Ramakrishna, S. 2010. Preparation and electrochemical studies of electrospun TiO<sub>2</sub> nanofibers and molten salt method nanoparticles *Elect Act.*, 55:3109-3117.
- [24] Ruby Chauhan., Ashavani Kumar., Ram Pal Chaudhary. 2011. Structural and optical characterization of Ag-doped TiO<sub>2</sub> nanoparticles prepared by a sol–gel method. *Res. Chem Intermed.*, DOI 10.1007/s11164-011-0475-8.
- [25] Bin Zhao., Yu-Wen Chen. 2011. Ag/TiO<sub>2</sub> sol prepared by a sol–gel method and its photocatalytic activity. *Journal of Physics and Chemistry of Solids*, 72: 1312–1318.

\*\*\*\*\*